JOURNAL OF MATERIALS SCIENCE **37** (2002) 2591 – 2596

Effect of microgravity on optical degradation in heavy metal fluoride glasses processed on the CSAR-II sounding rocket

S. VARMA
Supan Technologies Inc., 1877 Chaine Court, Orleans, ON, Canada K1C 2W6
E-mail: supantech@sprint.ca

S. E. PRASAD
Sensor Technology Ltd., 20 Stewart Road, P.O. Box 97, Collingwood, ON, Canada L9Y 3Z4

A. AHMAD, T. A. WHEAT
MTL/CANMET, Natural Resources Canada, 405 Rochester St., Ottawa, ON, Canada K1A 0G1

The optical properties of heavy metal fluoride (HMF) glasses degrade during the fibre drawing process due to undesired micro-crystal formation. Since gravity-driven density segregation is believed to be a major cause for homogeneous nucleation in viscous glasses during their ground-based processing, use of microgravity during such processes should minimize micro-crystal formation and resulting optical degradation. Our research on HMF glasses has been aimed at seeking experimental evidence to support this hypothesis. Earlier results from our experiments on the T-33 aircraft and the CSAR-I sounding rocket had indicated that microgravity helps in reducing crystallization in HMF glasses during their heat treatment at temperatures above 325°C. This temperature is very close to the fibre drawing temperature range of 300–320°C in these glasses, and implies that crystal nucleation and optical degradation may occur during fibre drawing. Therefore, the CSAR-II sounding rocket experiments were conducted on HMF glass samples at processing temperatures within the fibre drawing region. The results of CSAR-II sounding rocket experiments are in tune with the earlier findings and indicate that microgravity helps in reducing optical degradation in HMF glasses during their processing at temperatures in the fibre drawing region. © *2002 Kluwer Academic Publishers*

1. Introduction

Fibre optic telecommunication is one of the fastest growing technology sectors. Silica fibres are currently used in optical communication systems, which have attained their theoretically predicted loss of 0.15 dB/km. The capacity and speed of data communication through optical fibres are rapidly increasing. Thus, new materials with significantly lower losses will be desired in the future. Heavy metal fluoride (HMF) glasses are amongst the most promising optical fibre materials for future applications due to their predicted ultra-low loss limit of 0.001 dB/km [1]. Their high transparency in the mid-infrared region also makes them attractive for laser power delivery in laser surgery, infrared spectroscopy, remote sensing, and other applications [2].

HMF glass fibres are produced by a two-step process involving glass synthesis by a melt-quenching process, followed by fibre drawing from a reheated viscous glass preform. Unfortunately, the conventional process techniques have failed to realize the predicted low losses in HMF glasses and fibres. The lowest reported loss in a HMF glass fibre is 0.65 dB/km [3], which is still higher than the loss achieved in a commercial silica fibre. Higher than predicted losses in HMF glasses are produced by ionic absorption [4], excess scattering from bubbles, impurities and other defects [5], and excess scattering from phase separated regions [6] and micro-crystals [7]. Although process refinements over years have minimized ionic absorption and scattering losses due to bubbles, impurities and other defects, they have failed to eliminate phase separation and micro-crystal formation during HMF glass synthesis and fibre drawing.

Gravity-driven density segregation is believed to be the primary cause for phase separation and homogeneous nucleation in HMF glasses, while contamination from the processing container is the main cause for heterogeneous nucleation. Thus, microgravity containerless processing may minimize phase separation and micro-crystal formation during HMF glass synthesis and fibre drawing.

HMF glass synthesis has yet to be attempted in microgravity. However, scientists in France have reported synthesis of HMF glasses by a ground-based containerless process using a gas film levitator. Low scattering losses of 0.015 dB/km have been reported in these

samples [8]. Although low-loss fibres were predicted from these low-loss HMF glass preforms, they have not materialized. Optical degradation in HMF glasses during the fibre drawing process has been reported by some other scientists [9], and this may be the reason why low-loss fibres have not been realized from such low-loss glass preforms.

Our research has been aimed at studying the effect of microgravity on crystallization and optical degradation in HMF glasses during their heat treatment for fibre drawing. Our earlier experiments on the T-33 aircraft [10, 11] and the CSAR-I sounding rocket [12, 13] indicated that microgravity helps in reducing crystallization during heat treatment of HMF glasses at temperatures above 325°C. A similar effect of microgravity on HMF glass processing was also obtained by a NASA scientist during his experiments on the KC-135 aircraft and a sounding rocket [14, 15]. Ground-based crystallization at temperatures around 325°C implies that crystal nucleation in HMF glasses may occur at slightly lower temperatures in the fibre drawing region of 300–320°C. The CSAR-II sounding rocket experiments on HMF glasses were aimed at optical degradation studies in this temperature region. This paper describes the payload, provides experimental details and presents results obtained from these experiments.

2. Payload description

The payload used earlier for the CSAR-I sounding rocket experiments was refurbished and reused for the CSAR-II sounding rocket experiments. The CSAR-I payload has already been described elsewhere [12, 13]. Although the basic design and operation remained the same, many modifications were made to the CSAR-I payload to make it more suitable for the CSAR-II sounding rocket experiments.

The CSAR-II experiments were aimed at processing HMF glass samples at different temperatures in a narrow range of 300–320°C. This required excellent control, stability, reproducibility and uniformity in temperatures across the furnaces and the glass samples. Some modifications and refurbishment were dictated by the damage to the electrical connectors of the payload after the CSAR-I rocket flight and the desire to improve the reliability of the payload for the next rocket flight. A reduction in overall weight of the payload was dictated by the Canadian Space Agency in order to improve the microgravity duration for the CSAR-II rocket flight.

The payload modifications included: new furnaces with lower thermal mass and lower power consumption, new PID temperature controllers, new sample holders with attached thermocouples, additional electronics associated with measuring and recording six sample temperatures, a new set of internal batteries with reduced capacity, new electrical wiring and connectors, and changes to the countdown sequence to facilitate complete shutdown of the payload upon re-entry.

The payload consisted of six pairs of stacked annealing and processing furnaces. These isothermal furnaces were differentially wound on fired machinable ceramic cores to provide a temperature uniformity of ±1°C over a 50 mm long flat temperature zone at a maximum operating temperature of 450°C. The redesign resulted in a 6 Kg reduction in the weight of the furnace rack and lower operating temperature allowed the power requirement for each furnace to drop to 30 W. This also enabled us to reduce battery capacity, which resulted in an additional saving of 16 Kg in battery weight. The temperature of each furnace was controlled within ±1°C of the set point by a dedicated Dowty TC-48 PID controller. This produced excellent control, reproducibility and stability in temperatures of furnaces and samples.

Each annealing and processing furnace pair processed one set of undoped and rare-earth-ion-doped HMF glass samples. These glass samples were sealed in a fused silica capsule and placed in a copper sample holder. Six such sample holder assemblies were used for simultaneously processing twelve HMF glass samples in six pairs of annealing and processing furnaces. Each HMF glass sample was typically 15–20 mm (L) × 4 mm (D) and the two samples in each capsule were separated by fused silica spacers. In order to achieve faster heating and cooling of the samples, the sample holders were redesigned with lower thermal mass and fabricated with highly conducting copper material.

The sample temperatures were measured directly by six thermocouples, each attached to a sample holder, and recorded throughout the process cycle. The electronics associated with measuring and recording sample temperatures was added to the system. The on-board data-logger and telemetry links were reconfigured to include recording of sample temperatures from these six additional thermocouples. The whole payload was rewired and new electrical connectors were used to improve payload reliability. The payload was subjected to extensive testing and flight qualification due to the changes made to its structure and configuration.

3. Experimental details

3.1. Glass synthesis

HMF glass samples were synthesized in the ZBLAN (ZrF_4, BaF_2, LaF_3, AlF_3, NaF) glass system using a conventional melt-quenching process, which has been described elsewhere [10–13]. However, glass synthesis facilities and process technology were refined to improve the optical properties of HMF glasses produced for the CSAR-II rocket experiments compared to those produced earlier. ZBLAN glass samples were synthesized in three compositions, namely L4 (4%LaF_3) L6 (6%LaF_3) and L8 (8%LaF_3), which are given in Table I.

Rare-earth-ion-dopants (PrF_3, ErF_3 or NdF_3) were added to these base compositions at concentration levels of 500–1500 parts per million by weight

TABLE I Composition of ZBLAN glasses

	Composition in mol%		
Raw materials	L4	L6	L8
ZrF_4	53	51.5	50
BaF_2	20	19.5	19
LaF_3	4	6	8
AlF_3	3	3	3
NaF	20	20	20

(ppmw), whenever Pr, Er or Nd doping was desired. Three cylindrical HMF glass preforms of about 4 mm (D) × 60 mm (L) size were produced in each glass synthesis run.

The preforms were visually inspected for crystallization, bubbles, voids, and particulate matter inclusions. A thin film of graphite was transferred from the mould onto the surface of these preforms, which was removed by mechanical polishing. HMF glass samples of 15–20 mm length were sliced off from these preforms. Only samples free from visual defects were used in the experiments.

3.2. The CSAR-II rocket flight experiments

The CSAR-II rocket was launched in December 1994 from the White Sands Missile Range in New Mexico, USA. The carrier was a two-stage Black Brant-9 rocket built by Bristal Aerospace Limited, which carried five research payloads into space to achieve a microgravity duration of about seven minutes. The rocket launch and the flight went smoothly and the payloads were recovered in good condition after landing.

Undoped, Pr-doped and Nd-doped ZBLAN glass samples in L4 and L8 compositions were used for the actual degradation studies on the CSAR-II sounding rocket. The doping level for PrF_3 or NdF_3 was 1500 ppmw. Prior to the rocket launch, a set of six HMF glass sample assemblies, each consisting of one undoped and one rare-earth-ion-doped HMF glass sample sealed in fused silica capsules, were loaded into the six sample holders. These samples were preheated for 30 minutes prior to the rocket launch. The annealing temperature was set and maintained at 250°C during this period. The processing furnaces were also preheated at their set-points in the range of 310–340°C. The rocket launch and payload operation during the CSAR-II rocket mission were similar to the CSAR-I rocket mission described elsewhere [12, 13], except that the payload was shut down as soon as the rocket reentered the earth's atmosphere during the CSAR-II mission. The samples were recovered in good condition and sent for characterization and analyses.

The on-board data-logger and telemetry link provided records of furnace temperatures, sample temperatures, top and bottom limit switch activation, 0-g and 300 sec event signals, battery voltages and currents, etc., throughout the rocket flight. Analyses of these confirmed that the payload performed well and all the sample pairs were processed. The actual heating profile for each sample pair was recorded for the CSAR-II rocket flight experiments. The sample temperatures were found to slowly increase from the annealing temperature towards the pre-set processing temperature, but they did not reach the preset temperature even by the end of the processing cycle. The maximum sample temperatures recorded during the processing were treated as the processing temperatures, which were in the range of 310–320°C.

3.3. The CSAR-II ground-based experiments

The CSAR-II ground-based experiments were conducted after analysing the payload performance data recorded by the on-board data-logger during the rocket flight. These ground-based samples were processed on the CSAR-II payload using the same furnace pairs and the same sample heating profiles that were used and recorded during the CSAR-II rocket flight. However, the ground-based sample heating profile for one pair of samples (in holder #6) did not match the sample heating profile recorded for the same sample holder during the rocket flight, and these samples were not included in the studies.

It is to be noted that HMF glass samples processed during the CSAR-II rocket flight were obtained from the same glass synthesis run that provided the samples processed on the ground using the same heating profile and corresponding untreated reference samples.

3.4. Sample characterization

Differential thermal analysis (DTA) plots for undoped and rare-earth-ion-doped HMF glass samples were obtained using a Shimadzu DTA 50 system to see the effect of doping on the glass transition, on-set of crystallization and melting temperatures. The sample size was about 10 mg, N_2 flow was 40 ml/min, the temperature range was from 100–500°C, and the sample heating rate was 5°C/min.

Refractive index measurements were done on various undoped and rare-earth-ion-doped HMF glass samples to assess the effect of doping on the same. A preform analyser from York Technology, Model P102, was used for refractive index measurements.

Transmission spectra on HMF glass samples were obtained by a Perkin-Elmer Lambda-19 ultraviolet-visible-infrared spectrometer over a wavelength range of 0.20–3.0 μm, while a Perkin-Elmer 1600 series Fourier Transform Infrared (FTIR) spectrometer was utilized over the range of 2.0–10.0 μm. The sample compartment was purged by dry nitrogen to avoid absorption of moisture and carbon dioxide in the room.

The optical loss (attenuation) in HMF glass samples was estimated at desired wavelengths from the values of sample length, refractive index and transmittance at that wavelength. The attenuation was estimated by calculating Fresnel reflection (R) and Fresnel loss (F_R) at each face of the sample, calculating total sample attenuation (A) from transmission (T), and finally calculating attenuation (α) for the glass by making Fresnel loss corrections to total sample attenuation from both faces of the sample. The following equations were used in these calculations:

$$R = [(n_1 - n_2)/(n_1 + n_2)]^2$$

$$F_R \text{ (dB/facet)} = 10 \log [1/(1 - R)]$$

$$A \text{ (dB)} = 10 \log (1/T)$$

$$\alpha \text{ (dB/m)} = [\mathrm{A} - 2(F_R)]/L$$

where n_1 is the refractive index of the glass sample, n_2 is refractive index for air and L is length of the sample in metres. The minimum attenuation in the glass samples was estimated from maximum transmission, which was usually achieved in the infrared region of 4–5 μm due

to the absence of strong absorption from dopants or impurities in that region.

Rare-earth-ion-dopant concentration in HMF glass samples (in ppm) was estimated from various absorption peaks in the absorption spectra, which were derived from the transmission spectra. The attenuation at an absorption peak was calculated from the background transmission (by using the above equations). The attenuation was then divided by the absorption peak height in dB/km per ppm [16]. The values obtained from various absorption peaks were averaged.

4. Results and discussions

4.1. Thermophysical properties of as-synthesized HMF glasses

Thermophysical characterization of undoped and rare-earth-ion-doped ZBLAN glasses (as-synthesized) by DTA indicated that rare-earth-ion-doping did not affect the temperatures for glass transition, onset of crystallization or melting in these glasses. Irrespective of ZBLAN glass composition, dopant ion or dopant concentration, these measurements at a sample heating rate of 5°C/min indicated the glass transition to be around 260°C and the onset of crystallization to be around 340°C. Our earlier research had indicated that at a slow heating rate of 2°C/min during DTA measurements, and during steady-state glass processing experiments, the onset of crystallization in undoped ZBLAN glasses was around 320°C [13]. Therefore, rare-earth-ion-doped ZBLAN glasses should also have the same onset of crystallization temperature. The melting temperature was around 420°C for ZBLAN glasses in L4 composition and around 440°C for ZBLAN glasses in L8.

4.2. Optical properties of as-synthesized HMF glass samples

Refractive index measurements on undoped and rare-earth-ion-doped ZBLAN glass samples indicated that neither the glass composition nor the rare-earth-ion-doping had any significant effect on the refractive index of these glasses. The refractive index was around 1.492 for undoped and around 1.493 for rare-earth-ion-doped ZBLAN glasses.

ZBLAN glass samples for this research were synthesized in a controlled environment of a Clean Room. Facility improvements and process refinements significantly improved the optical properties of these glasses. In undoped ZBLAN glasses, the transmission was fairly uniform over a wavelength region of 0.3–5.5 μm. Some shallow absorption peaks due to one or more ionic impurities, such as hydroxyl ions (at 2.8 μm), carbon (at 3.4 μm), carbon dioxide (at 4.25 μm) and carbon monoxide (at 4.75 μm), were detected in the transmission spectra of these undoped glasses. Rare-earth-ion-doped ZBLAN glass samples had similar infrared transmission, but also had absorption peaks in visible-infrared region due to the presence of dopant ions. Moreover, their transmission was affected by the type of dopant ion and its concentration. The maximum transmission in rare-earth-ion-doped ZBLAN glasses was usually obtained in the wavelength region of 4–5 μm, since that region was usually free from strong absorption peaks. Fig. 1 shows an infrared transmission spectrum for a typical Pr-doped (1500 ppmw) ZBLAN glass sample in L8 composition. The maximum transmittance in undoped and rare-earth-ion-doped ZBLAN glasses was usually in the range of 90–95%, compared to about 85% in ZBLAN glasses produced during earlier research [12, 13].

TABLE II Effect of rare-earth-ion-doping on transmission and attenuation in ZBLAN glasses

Doping fluoride cone. (ppmw)	Av. dopant conc. (ppm)	L (mm)	T-max (%)	α-min (dB/m)
ErF_3 (500)	Er (414)	9.8	80.7	60
ErF_3 (1000)	Er (690)	9.8	83.7	44
ErF_3 (1500)	Er (1136)	10	87.8	20
PrF_3 (500)	Pr (354)	9.8	71.4	114
PrF_3 (1000)	Pr (745)	9.8	84.1	42
PrF_3 (1500)	Pr (892)	10	92.2	1
NdF_3 (500)	Nd (328)	9.8	82.6	50
NdF_3 (1000)	Nd (671)	9.8	95.5	<1
NdF_3 (1500)	Nd (1000)	10	82.6	49

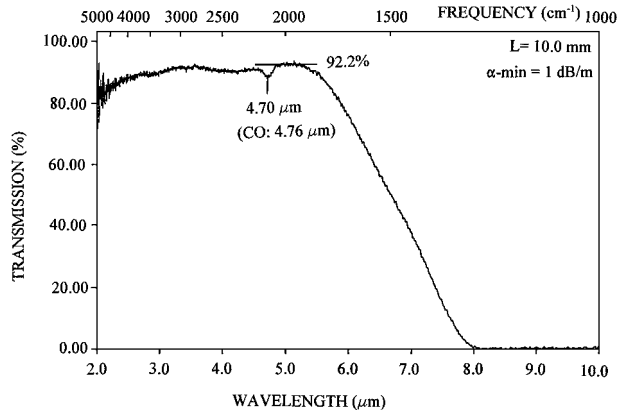

Figure 1 Infrared transmission spectrum of a Pr-doped ZBLAN glass sample.

The maximum transmission was used to calculate minimum attenuation in these glasses. These values for various rare-earth-ion-doped ZBLAN glass samples are presented in Table II. The data indicated that maximum transmission and minimum attenuation in these glasses were affected by the dopant ion and doping concentration. The lowest attenuation in Er-doped glasses was 20 dB/m at a doping level of 1500 ppmw, while in Pr-doped and Nd-doped glasses it was about 1 dB/m at a doping level of 1500 ppmw and 1000 ppmw respectively.

Fig. 2 shows dopant absorption peaks in the transmission spectrum of the Pr-doped ZBLAN glass, whose infrared transmission spectrum is shown in Fig. 1. An absorption spectrum for this sample in the visible region, which was derived from the transmission spectrum in Fig. 2, is shown in Fig. 3.

Such absorption spectra were used to calculate the dopant concentration in rare-earth-ion-doped ZBLAN glasses. The averaged dopant concentration calculated in various samples is also presented in Table II. These values agree qualitatively with the dopant concentration in raw materials.

TABLE III Effect of quench-anneal temperature on transmission and attenuation in ZBLAN glasses

Sample description	Quench-anneal temp. (°C)	L (mm)	T-max (%)	α-min (dB/m)
L4, Undoped	300	8.83	91	7
L4, Undoped	310	8.9	84	47
L8, Undoped	300	8.8	86.1	35
L8, Undoped	310	7.73	79.7	83
L4, Pr-doped	300	8.87	92.8	1
L4, Nd-doped	310	7.6	84	54
L8, Pr-doped	300	9.8	84.1	42
L8, Nd-doped	310	8.85	73.2	114

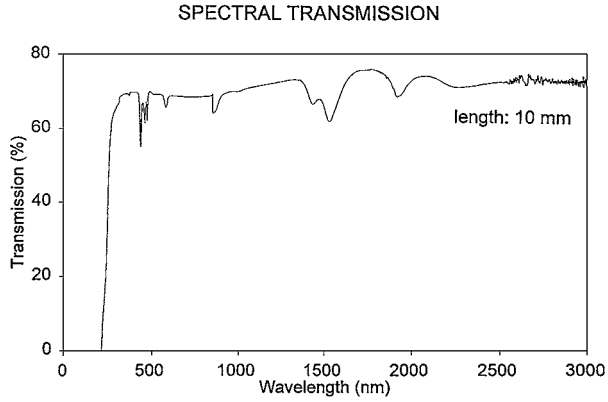

Figure 2 Ultraviolet-visible-infrared transmission spectrum of the Pr-doped ZBLAN glass sample.

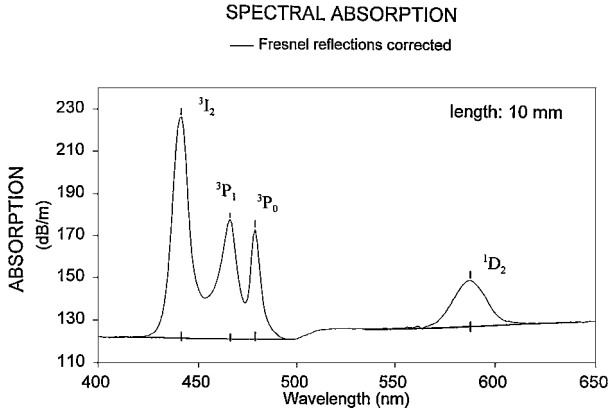

Figure 3 Absorption spectrum of the Pr-doped ZBLAN glass sample in visible region.

When the quench-anneal temperature at the end of HMF glass synthesis process was increased from 300°C to 310°C, it had an adverse affect on the maximum transmission and minimum attenuation realized in these glasses. This can be seen from the data presented in Table III. Also, ZBLAN glasses in L4 composition generally produced higher transmission or lower attenuation compared to ZBLAN glasses in L8 composition for the same quench-anneal temperature.

4.3. The CSAR-II sounding rocket experiments

The sample heating profile for HMF glass samples processed in the sample holder #5 during the CSAR-II rocket flight is shown in Fig. 4. It matches well with the sample heating profile for the samples processed in the sample holder #5 during the ground-based experiments, which is shown in Fig. 5.

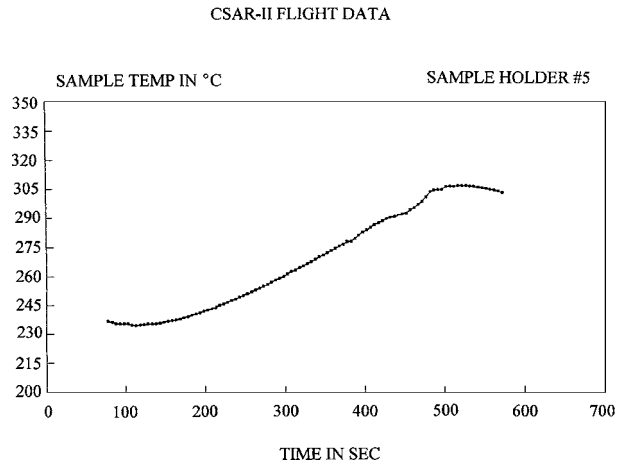

Figure 4 Temperature profile of the sample holder #5 during the CSAR-II microgravity experiments.

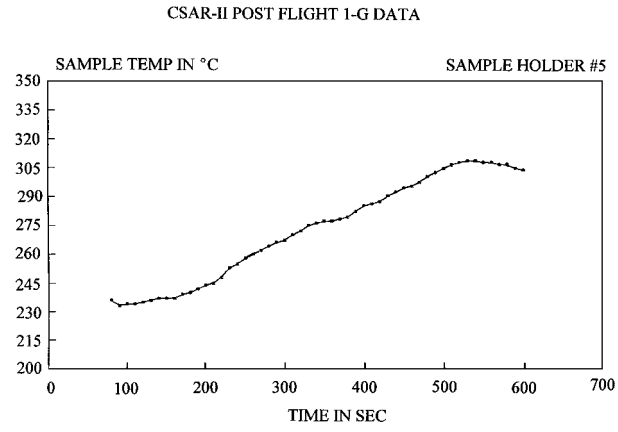

Figure 5 Temperature profile of the sample holder #5 during the CSAR-II ground-based experiments.

Similar matches were realized in the sample heating profiles for all other samples, except those in the sample holder #6 which were discarded from the study. These profiles indicate that the samples were processed around the final processing temperature for only a couple of minutes since most of the processing time was utilized by the samples in going from the annealing temperature to the processing temperature.

Table IV summarizes results of optical degradation observed in HMF glass samples during the CSAR-II rocket flight as well as ground-based experiments. The transmission and attenuation in as-synthesized glass samples were used as a reference. These results indicated that in spite of the short processing time of a couple of minutes near the final processing temperature in the range of 310–320°C, all samples showed optical degradation after their processing in microgravity or on the ground. This optical degradation is believed to be due to crystal nucleation during the viscous processing of these glasses. It is to be noted that the optical degradation in ZBLAN glass samples processed in microgravity at a temperature of 310°C was significantly lower than the degradation observed in the samples processed

TABLE IV Effect of microgravity and ground-based processing on optical degradation

Sr. no.	Sample details	Process temp. (°C)	As-synthesized		Processed in microgravity		Processed on the ground	
			T-max (%)	α-min (dB/m)	T-max (%)	α-min (dB/m)	T-max (%)	α-min (dB/m)
1	L4, undoped	310	91	7	82.2	58	48.7	364
2	L4, undoped	310	91	7	80.7	76	57.7	265
3	L4, Pr-doped	310	92.8	1	86.1	35	65.9	273
4	L4, Pr-doped	310	92.8	1	86.4	38	56.3	276
5	L8, undoped	315	79.7	83	47.2	378	66	191
6	L8, Nd-doped	315	73.2	114	48.6	314	56.6	278
7	L4, undoped	320	84	47	Cryst.	Cryst.	44.7	415
8	L8, undoped	320	86.1	35	Cryst.	Cryst.	N/A	N/A
9	L4, Nd-doped	320	84	54	Cryst.	Cryst.	N/A	N/A
10	L8, Pr-doped	320	79.5	83	Cryst.	Cryst.	N/A	N/A

on the ground at the same temperature. This indicates that microgravity helped in minimizing optical degradation in HMF glass samples processed at 310°C.

HMF glass samples processed in microgravity at 320°C showed extensive crystallization, probably due to high gravity exposure of these samples during the rocket's re-entry while the samples were hot enough to crystallize at such gravity levels. Similar effect of high gravity exposure was also noticed during the CSAR-I rocket experiments [13]. Crystal nucleation due to high gravity exposure could also be the reason for observing slightly higher optical degradation in HMF glass samples processed in microgravity at 315°C compared to those processed on the ground. Thus, future rocket experiments should ensure that HMF glass samples are rapidly cooled below this critical temperature before the rocket's re-entry to minimize adverse effect of high gravity exposure on these glasses.

5. Conclusions

The CSAR-II rocket experiments indicated that microgravity helps in reducing optical degradation in HMF glass samples during their re-heating to temperatures around 310°C. Since HMF glass fibres are drawn around these temperatures and optical degradation on the ground has been observed by many researchers, these findings are significant as they show the possibility of minimizing optical degradation during fibre drawing in microgravity.

High gravity exposure of samples during the rocket's re-entry can cause extensive crystallization in HMF glass samples, if the sample temperature remains close to the onset of crystallization temperature at this juncture. Thus the samples should either be rapidly cooled or quenched after their microgravity processing on sounding rockets. This problem is unique to rocket flights and would not be a concern during the future experiments likely to be done on space shuttle or space station.

Acknowledgements

The financial support for this research was provided by the Canadian Space Agency under the contract #9F007-3-6003/01-SR, which is greatly appreciated. We wish to acknowledge invaluable contribution made by the staff of Sensor Technology Ltd., specially M. Verghese, during payload modification, testing, integration, rocket launch and HMF glass processing on the payload. We also wish to thank the team from Bristol Aerospace Ltd. for its support during the payload testing, integration and rocket launch. The DTA measurements on HMF glasses were done at CANMET by G. McDonald, and we wish to thank him for the same. Finally we wish to thank A. Croteau and F. Chenard of the National Optics Institute, Ste-Foy, Quebec, for the optical measurements on HMF glass samples and analysis of optical results.

References

1. S. SHIBATA, M. HORIGUCHI, K. JINGUJI, S. MITACHI, T. KANAMORI and T. MANABE, *Electron. Lett.* **17** (1981) 775.
2. M. G. DREXHAGE, in "Halide Glasses for Infrared Fibreoptics," edited by R. M. Almeida (NATO ASI Series E: No. 123, 1987) p. 219.
3. S. F. CARTER, J. R. WILLIAMS, M. W. MOORE, D. SZEBESTA and S. T. DAVEY, *J. Non-Cryst. Solids* **140** (1992) 146.
4. T. NAKAI, Y. MIMURA, H. TOKIWA and O. SHINBORI, *Electron Lett.* **21** (1985) 625.
5. P. W. FRANCE, S. F. CARTER, C. R. DAY and M. W. MOORE, in "Fluoride Glasses," edited by A. E. Comyns (John Wiley and Sons, New York, 1989) p. 87.
6. L. BOEHM, K. H. CHUNG, S. N. CRICHTON and C. T. MOYNIHAN, *Mat. Sci. Forum* **19/20** (1987) 533.
7. S. F. CARTER, P. W. FRANCE, M. W. MOORE and J. R. WILLIAMS, *ibid.* **19/20** (1987) 511.
8. A. LOPEZ, P. BANIEL, P. GALL and J. GRANIER, in Proceedings of Spie Conference on Submolecular Glass Chemistry and Physics, Vol. 1591, edited by P. Bray and N. J. Kreidl (Spie, Bellingham, Washington, 1991) p. 191.
9. S. TAKAHASHI and H. IWASAKI, in "Fluoride Glass Fiber Optics," edited by I. D. Aggarwal and G. Lu (Academic Press, San Diego, 1991) p. 218.
10. S. VARMA, S. E. PRASAD, I. MURLEY and T. A. WHEAT, in Proceedings of Spacebound'91, Ottawa, May 1991 (CSA, 1991) p. 248.
11. S. VARMA, S. E. PRASAD, A. AHMAD and T. A. WHEAT, *J. Mater. Sci.* **36** (2001) 4551.
12. S. VARMA, S. E. PRASAD, A. AHMAD, T. A. WHEAT and K. ABE, in Proceedings of Spacebound'92, Ottawa, May 1992 (CSA, 1992) p. 109.
13. S. VARMA, S. E. PRASAD, A. AHMAD and T. A. WHEAT, *J. Mater. Sci.* **36** (2001) 2027.
14. D. S. TUCKER, NASA Technical Memorandum TM-108461, Marshall Space Flight Centre (NASA, 1994).
15. D. S. TUCKER, G. L. WORKMAN and G. A. SMITH, *J. Mater. Res.* **12**(9) (1997) 2223.
16. P. W. FRANCE *et al.*, in "Fluoride Glass Optical Fibers" (Blackie, Glasgow, 1990).

Received 12 January 2000
and accepted 13 February 2002